Early Detection of Esca Disease in Asymptomatic Vines by Raman Spectroscopy

Camilla Baratto, *Member, IEEE*, Gina Ambrosio, Guido Faglia, and Massimo Turina

***Abstract*—Early detection of esca disease in grapevines is fundamental to calibrating proper pesticide use in sustainable vineyard management systems. This article is a proof of concepts showing that the Raman spectroscopy (RS) combined with a chemometric analysis can be used as a nondestructive sensor to implement precision agriculture for early detection of the disease through a new biochemical marker. Symptomatic and symptomless branches from an esca-developing vine and from healthy esca-free vines from a vineyard were investigated by RS and chemometrics, using the final outcome of the specific disease syndrome as the final benchmark. As a result, the model is always able to correctly classify all the test samples, showing auspicious results to perform precision agriculture-based future therapeutic approaches.**

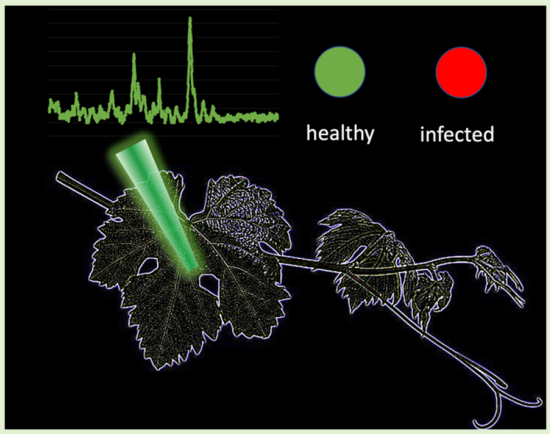

***Index Terms*—Chemometric, esca disease, precision agriculture, Raman spectroscopy (RS).**

I. Introduction

EARLY detection of plant pathogens is fundamental for preventing disease spread, limiting crop damage, and calibrating proper pesticide use in sustainable crop management systems. Objective and "nonoperator-dependent" diagnostic techniques must support the identification of pathogens by visual assessment. Esca disease is one of the specific diseases, part of the grapevine trunk disease complexes, which are currently a cause of significant concern for their increasing prevalence in most grapevine (*Vitis vinifera*) growing areas worldwide [1]. Esca itself is a significant concern in all wine-producing countries often with a tremendous economic impact [2]; the disease is associated with systematically diverse fungi (*Phaeoacremonium aleophilum, Phaeomoniella chlamydospora*, and *Fomitiporia mediterranea*). Such fungi can be present also in healthy plants [2], and their inoculation often does not reproduce the disease [3]. Therefore, the actual etiology is complex, and still to be unveiled, including yet to be identified environmental and microbiological components including the rest of the microbiota associated with grapevines [4]. New biochemical and physiological markers for this complex disease are, therefore, necessary.

Esca complex includes two typical severity levels of symptoms: the chronic form is called the grapevine leaf stripe disease (GLSD), whereas apoplexy consists of partial or complete sudden wilting of the vine; the wood underneath the bark has different shapes of necrosis/discoloration, and the most common is called the brown wood streaking (BWS). The first symptoms of esca on leaves appear as dark red (for red cultivars) or yellow (on white cultivars) stripes on the leaves, which eventually wilt and become necrotic. When the disease progresses, it causes dieback of the entire grapevine. Once symptoms are detected visually, it is already too late for a possible precision therapeutic intervention. It is, thus, of utmost importance to find a technique that allows for early monitoring

Manuscript received 14 August 2022; revised 22 September 2022; accepted 22 September 2022. Date of publication 10 October 2022; date of current version 30 November 2022. This work was supported in part by the sPATIALS3 project (ID 1176485), financed by the European Regional Development Fund under the Regional Operational Programme (ROP) of the Lombardy Region European Regional Development Fund (ERDF) 2014–2020—Axis I "Strengthen technological research, development and innovation"—Action 1.b.1.3 "Support for co-operative R&D activities to develop new sustainable technologies, products and services"—Call Hub. The associate editor coordinating the review of this article and approving it for publication was Prof. Mohammad Russel. *(Corresponding author: Camilla Baratto.)*

Camilla Baratto and Gina Ambrosio are with the PRISM Lab, National Research Council–National Institute of Optics (CNR-INO), 25123 Brescia, Italy (e-mail: camilla.baratto@cnr.it; gina.ambrosio@ino.cnr.it).

Guido Faglia is with the Department of Information Engineering, University of Brescia, 25133 Brescia, Italy, and also with the PRISM Lab, National Research Council–National Institute of Optics (CNR-INO), 25123 Brescia, Italy (e-mail: guido.faglia@unibs.it).

Massimo Turina is with the CNR-IPSP, Turin, 25133 Brescia, Italy (e-mail: massimo.turina@ipsp.cnr.it).

Digital Object Identifier 10.1109/JSEN.2022.3211616

of the disease before any symptomatic onset. Fluorescence tests were reported for chlorophyll-a detection, demonstrating that it can give warnings about symptom onset seven days before apoplexy of the plant [5], which is not enough to save the plant with a possible pesticide treatment [6]. Results obtained in the early detection of GLSD by multispectral images were very dependent on the period of observation and did not discriminate on the type of stress [7].

Raman spectroscopy (RS) is an emerging analytical technique that can be used to develop precision agriculture. The RS allows for confirmatory diagnosis of biotic [8] and abiotic stresses [9] on plants. For example, the RS was used for diagnostics of Huanglongbing (HLB) disease on both orange and grapefruit trees [10], as well as the detection and identification of various fungal and viral infections [11], [12], [13].

The Raman technique shows distinct advantages over established in vivo plant stress sensing techniques, such as reflectance spectroscopy [14], hyperspectral band remote sensing [15], chlorophyll fluorescence spectroscopy [16], IR thermal imaging, and terahertz time-domain spectroscopy. It offers earlier detection, biochemical selectivity, the ability to discriminate among multiple stress conditions, and the detection of initial defense responses. The Raman technique can detect changes in carotenoids and anthocyanins, which are impacted during the first line of defense responses of plants to biotic stress [8], [17], [18].

Unlike other plant-pathogen diagnostic techniques, such as enzyme-linked immunosorbent assay (ELISA) or polymerase chain reaction (PCR), specific for the fungal complex, the RS is a nondestructive technique that does not require protein or nucleic acid sample extraction. In the case of esca disease, the detection of early symptoms caused by xylem necrosis localized under the bark would require peeling of the bark itself, an invasive and destructive procedure. The RS would provide a possible alternative approach to symptom visualization, whereby we can detect alteration of the spectra in the distal part (leaves) caused by the release of specific chemicals associated with the disease or detect changes in the leaf metabolomic fingerprint due to the specific plant response.

Spectral data, such as the one obtained by RS, are often of high dimensionality, and the variables (i.e., wavenumbers) tend to be correlated with each other (i.e., collinearity). The partial least squares (PLS) algorithm was first introduced for regression tasks and then evolved into a classification method known as a PLS-discriminant analysis (PLS-DA), which has been widely used for predictive modeling. Theoretically, the PLS-DA combines dimensionality reduction and discriminant analysis into one algorithm and is especially applicable to modeling high-dimensional (HD) and collinear data as produced by RS [19].

To date, there is no report of RS for esca disease detection. This work combines the sensing capabilities of the RS technique and the chemometric analysis in order to develop a nondestructive analyzer for early detection (before symptom onset) of the esca disease. To this aim, leaf samples from healthy plants and from symptomatic and symptomless shoots in diseased plants were analyzed by RS at the early stages of the appearance of clear symptoms of esca in the vineyard. Since the presence of the fungi themselves is not a specific marker for the disease, at the moment, only the final symptomatic outcome of the specific disease syndrome was used as the final benchmark.

The outcomes of this preliminary investigation are very promising to perform precision agriculture-based future therapeutic approaches.

II. Materials and Methods

A. Plant Sample Collection

A field of grapevines (CV. Marzemino) in Brescia province (GPS 45.524403, 10.518457), known for its history of esca disease symptoms, was monitored for specific symptomatology every week from mid-May 2021. As a result, a specific area inside the vineyard was identified with clear early esca symptom development in mid-June. A single-point sample collection (28 June 2021) was organized in the heavily hit section of the vineyard. At the collection time, healthy vines (confirmed healthy throughout the later season until fall) shared space with entirely symptomatic vines (sometimes quickly developing a typical apoplectic syndrome) and with vines that showed symptoms limited to one branch (later developed in an entirely symptomatic vine). Different shoots representing these three types were brought to the laboratory sealed in plastic bags and analyzed 24 h after collected by RS.

B. Raman Spectroscopic Measurements

The Raman spectra were acquired from symptomatic and symptomless leaves from diseased and healthy plants. In the case of diseased vines, leaves without symptoms and leaves with red stripes were tested. The leaves were taken randomly from the canopy and rinsed with water before testing to remove possible pesticide residues. Wider and smaller leaves were considered with no differentiation observed in the results. At least two leaves were selected for each plant, and six Raman spectra were acquired on the top of each leaf by using a micro-Raman modular system by Horiba (Horiba, Kyoto, Japan), equipped with a single monochromator (iHR320) and Peltier cooled charge coupled device (CCD) camera (Horiba, Kyoto, Japan). To allow investigation on nonflat leaves, the acquisition was performed with a 50× long-working distance objective with a numerical aperture (NA) of 0.55; the focused area is on the order of 2 μm. In order to avoid subsampling [20], several points were tested in each leaf.

As for excitation, we used 532 nm from a solid-state laser: to minimize the fluorescence background of Raman spectra and to avoid heating of fresh samples, a very short exposure time was employed (2 s for three accumulations) as permitted by 600-g/mm grating (the lower resolution we use, the higher the signal we obtain with the same parameters; the resolution is 4 cm^{-1}). The system was calibrated using a silicon substrate at 520.5 cm^{-1} before measurements.

C. Chemometric Analysis of Raman Spectra

A chemometric analysis was conducted using the Classification toolbox for MATLAB, a collection of MATLAB modules for classification (supervised pattern recognition) through multivariate models [19]. Spectra were preprocessed

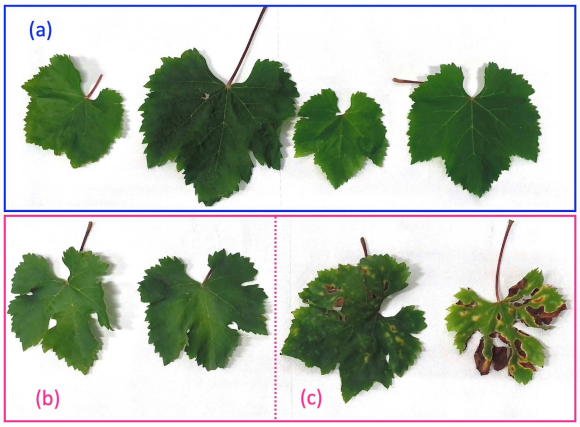

Fig. 1. Images of the leaves taken from (a) healthy vine; (b) infected vine, branch without symptoms; and (c) infected vine, branch with symptoms.

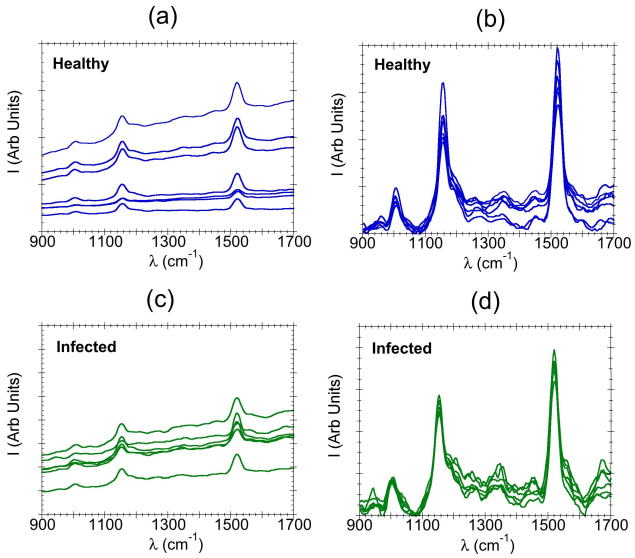

Fig. 2. Raman spectra of the leaves acquired before background removal and after background removal. Spectra were acquired in different places randomly selected among green areas of the leaves. (a) and (b) Taken on a healthy leaf. (c) and (d) Taken on a symptomatic leaf of an infected vine.

by Savitsky–Golay smoothing (11 points, polynomial order 3), removing random shift of the baseline offset by asymmetric least-squares baseline correction [21], [22]. The PLS-DA models were then used to determine RS sensitivity and specificity of esca disease infection recognition.

In a classification task, the output variables are categorical. The binary classification problem was implemented through the PLS-DA algorithm: output was recoded as two columns; one for each possible state, consistently assigning for each class (from the healthy vine and the diseased vine) 1 or 0 if belonging or not to the class, respectively (the two columns are complementary to one).

III. Results and Discussion

Fig. 1 shows the comparison of the leaves taken from a healthy vine and from an infected vine. The leaves from infected vine show symptomatic leaves [Fig. 1(c)] with red stripes typically associated with esca. Nevertheless, asymptomatic leaves taken from unaffected branch from the same vine [Fig. 1(b)] are indistinguishable from the ones taken from the healthy vines, shown in Fig. 1(a). In this research, only the symptomatic evaluation of the outcome of the specific disease syndrome is used as the final benchmark for the disease. It has been demonstrated that the biotic stress induced a variation in carotenoid content near the region of the symptoms [23], generating a variation in the Raman spectrum acquired on discolored/necrotic regions. Our scope is to investigate if the carotenoid variation is present also in the case of symptomless foliage coming from an infected plant. So, the Raman spectra were acquired on green areas of leaves for either healthy or diseased plants.

The Raman spectra acquired on healthy and on infected (symptomatic) leaf, in the range of 900–1700 nm, are shown in Fig. 2. The raw data without correction, acquired in the green area of leaves, are shown in Fig. 2(a) and (c); they are differently affected by fluorescence. The corresponding spectra after background/fluorescence removal and pretreatment described in Section II-C are shown in Fig. 2(b) and (d). Many preprocessing steps have been implemented: best results were obtained by applying vector normalization (two norm, length =1) to correct different scales across each sample spectra, followed by each variable (response at a given lambda for all samples) mean centering.

TABLE I
Raman Band Assignments for Carotenoid in Plants

Band (cm^{-1})	Vibrational assignments	Type of carotenoid	Ref
1005		β-carotene	[18]
1008	τ (CH_3)	Lutein (standard), α-carotene	[25]
1005		-	This work
1156-1157		β-carotene	[25] , [18]
1157	ν (C–C)	Lutein (standard)	[23]
1157		α-carotene	[23]
1156-1158		Healthy-unhealthy	This work
1510		Lycopene, tomato fruit	[22]
1515		β-carotene (standard)	[25]
1517		Capsanthin, pepper fruit	[22]
1520 - 1522	ν (C=C)	Healthy-unhealthy	This work
1521		α-carotene	[25]
1522		Lutein (standard)	[25]
1524		β-carotene	[25]
1527		carotenoids	[13]

In the literature, the characteristics peaks of carotenoids are observable at 1006 cm^{-1} (C–H bending), 1158 cm^{-1} (C–C stretching), and 1522 peak (C=C stretching) [18], [24]. The assignment of bands of the carotenoid peaks is also summarized in Table I. The position of the C=C stretching vibration could be used to determine the carotenoid involved in the process, for example, capsanthin occurs at 1517 cm^{-1} in

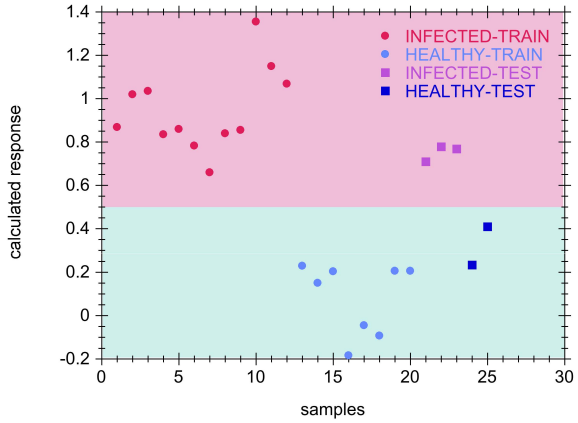

Fig. 3. Output for infected class (data for healthy are the complementary to 1 for each sample) of all the samples. Each sample is associated with the class whose output is greater, that is, samples with values greater than 1/2 are classified as infected (pink area) and samples with values lower than 1/2 as healthy (light blue area); 100% correct classification is obtained.

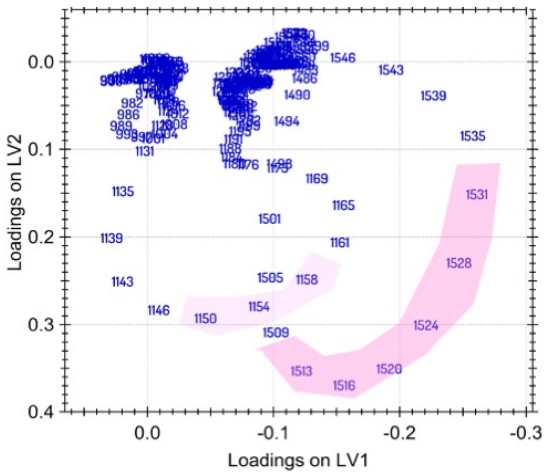

Fig. 4. Loadings on the first two LVs retained in the PLS-DA model. The two peaks at 1155 and 1520−highlighted in pink−are responsible for resolving the two classes.

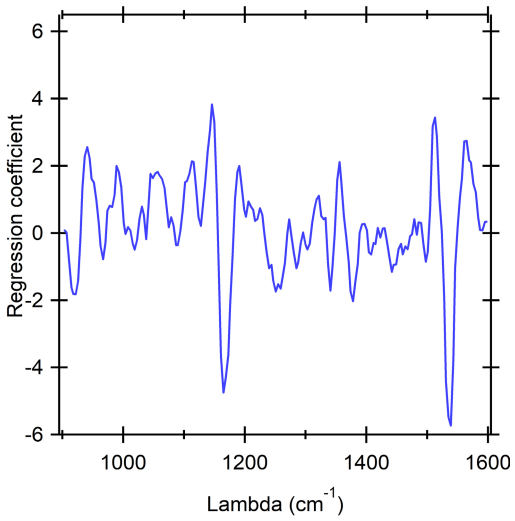

Fig. 5. Regression coefficients for samples from esca-affected plants. The coefficients for healthy are for any variable the opposite (given the classes are two).

pepper fruit and lycopene at 1510 cm^{-1} in tomato fruit, while β-carotene is at 1524 cm^{-1} in tomato fruit. Nevertheless, the peak position is also influenced by the plant species considered (standard β-carotene is at 1515 cm^{-1} instead of 1524 cm^{-1}, and standard lutein occurs at 1522 cm^{-1} [23], [25]). Moreover, the wavenumber variation is small compared with the resolution of the present experiments.

The peaks observed in our experiment−assigned to total carotenoids−have some variability, dependent also on the status of the plant (infected or healthy): peak at 1005 cm^{-1} is visible but very small (C–H bending). For the infected leaf [Fig. 2(c)], the mean values of the peaks at 1158 cm^{-1} (C–C stretching) and 1522 cm^{-1} (C=C stretching) are shifted to lower wavenumber, namely, 1156 and 1520 cm^{-1}. Given the size of the dataset, the detection of such a small shift to lower wavenumbers and its connection to infection was only made possible by applying the chemometrics techniques.

As output variables for the classification, we identified only two classes: healthy and infected, independently of the presence of symptoms. In this way, we can test if healthy and esca-diseased vines can be distinguished irrespective of the symptomatology of the samples. The best results were obtained by cutting out the wavenumbers outside the 900–1600-cm^{-1} range.

As for dimension reduction, we cross validated the training set with the "leave-one group-out" (given the small size of the set), using subsets for cross validation corresponding to one plant at a time. The root mean-squared error (RMSE) was the figure of merit used to assess classification model quality; we determined as four the optimal number of latent variables (LVs). The presence of outliers in the model has been evaluated by means of Q residuals and Hotelling's T2. All the data lie inside the 95% confidential interval of both features, confirming the quality of the model and the choice of LVs. As the last step given that the output of the PLS-DA is continuous variables, due to the small size of the dataset, we selected a naïve decision rule (DR) against other novel DRs (probability density function) by associating each sample to the class whose output was greater.

Fig. 3 reports the output for the infected class (data for health are complementary to 1 for each sample) of all the samples (red samples as infected and blue as healthy, while circles are train, and squares are test samples). Each sample is associated with the class whose output is greater, meaning that the samples with the values greater than 1/2 are classified as infected and the samples with the values lower than 1/2 as healthy. Notwithstanding the very simple DR, the model is always able to correctly classify all the test samples, implying that, in the confusion matrix, all entries would lie on the main diagonal.

In order to inquire and determine which part of the spectrum is responsible for such an efficient separation of healthy and infected plants, Fig. 4 reports the variables (lambdas) loadings on the first two LVs. Given that variables which are far

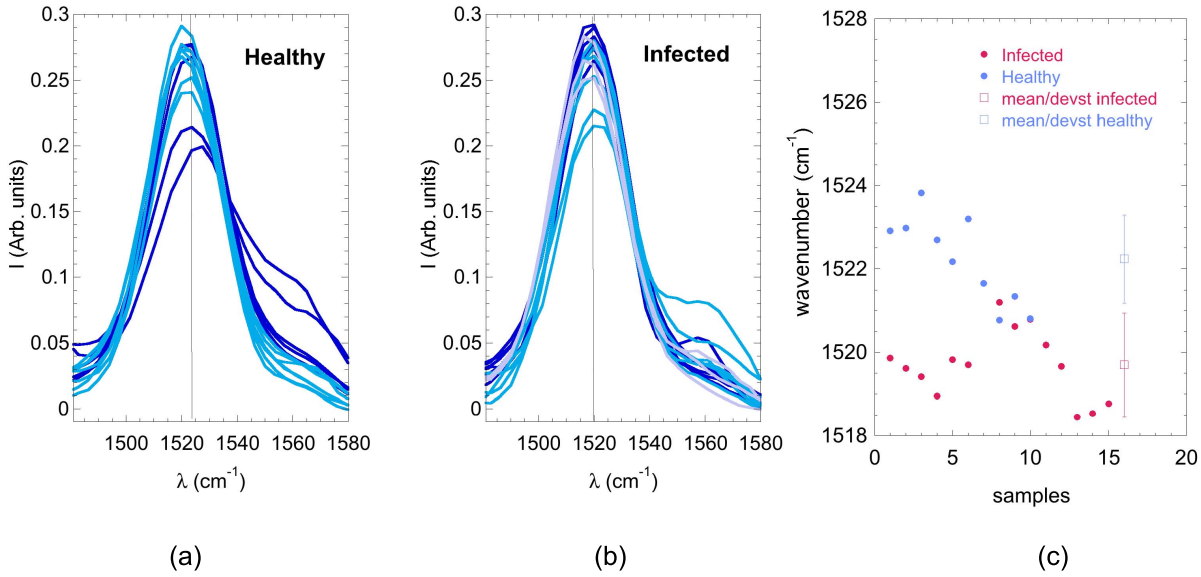

Fig. 6. Normalized data around C=C stretching of carotenoid acquired on (a) health leaves and (b) infected leaves: the center of the Lorentzian fit is shifted toward lower cm^{-1} for infected leaves. (c) Value of peak wavenumber obtained by Lorentzian fit, showing the mean and standard deviation for healthy and infected leaves.

from the origin weight more in building the response, it is evident that, as expected (both), the two peaks at 1156 and 1520 cm^{-1} – highlighted in pink – are responsible for resolving the two classes.

To assess how healthy or esca-diseased plants affect each of the two peaks, we resorted to the regression coefficients of the variables. The regression coefficients express, for each class, the contribution of raw input variables (lambda) in each of the latent PLS variables. Fig. 5 reports the regression coefficients for samples from esca-affected plants (the coefficients for healthy are for any variable the opposite). The asymmetric ringing of the regression coefficients around the two peaks, which is true in particular for the 1520 peak, suggested to have a closer detailed look at the data in order to find differences in the spectra for the two classes.

To further investigate the input variables that most influence the classification – related to the peak at 1520 cm^{-1}, we plotted, in Fig. 6, the normalized data around C=C stretching of carotenoid acquired on health leaves [Fig. 6(a)] and infected leaves [Fig. 6(b)]. We can observe that the center of the peak is shifted toward lower wavenumber for infected leaves. Fig. 6(c) reports the center wavenumber obtained from Lorentzian fit. The mean of all measurements is at 1519.7 cm^{-1} (approximated to 1520 cm^{-1}) for infected leaves and 1522.0 cm^{-1} (approximated to 1522 cm^{-1}) for healthy leaves, with a mean variation that is indeed below that of the instrument in the configuration used, but can be appreciated from the fit. A similar behavior has been observed on the C–C stretching vibration with a mean wavenumber at 1158.4 cm^{-1} (approximated to 1158) for healthy leaves shifting to a mean value at 1155.7 cm^{-1} (approximated to 1156) for healthy leaves.

In contrast to other approaches (such as Kennard–Stone sampling that ensures uniform distribution of samples), random sampling between training and test sets does not employ any principle in splitting the dataset. For this reason, as a good practice, we repeated the random sampling multiple times (i.e., iterative random sampling) in order to reduce unforeseen bias caused by the nonuniform sampling. Fig. 7 reports the regression coefficients following 50 repetitions of random sampling. Stability of the regression coefficients testifies the robustness of the model, which, notwithstanding the small size of the data set, does converge to very similar values of the parameters independently of which samples are picked up for the test.

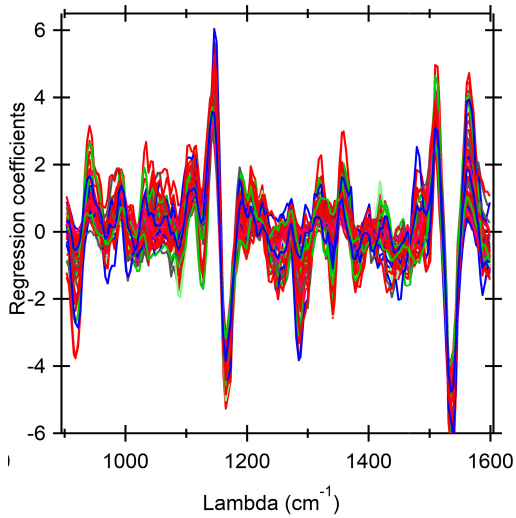

Fig. 7. Regression coefficients (infected) following 50 repetitions of random database splitting in train (80%) and test (20%) samples.

Quantitative and qualitative modifications of carotenoids due to esca disease are not surprising. Carotenoids and their derivatives (apocarotenoids) play a number of functions in plant physiology: in low light conditions, they act as antennae,

harvesting lights at wavelengths not absorbed by chlorophylls and feeding into photochemical reaction centers; in high light, they play a fundamental role in photoprotection. Their ecological role is also important, and it is expressed through their color or some volatiles derived from them. Finally, carotenoids are at the base of the synthesis of important plant hormones, such as abscisic acid and strigolactones. No specific study has looked at alterations in specific carotenoid and apocarotenoid contents upon esca-disease development, but the association to asymptomatic grapevine virus infection was recently shown [13]. Nevertheless, the concentration of carotenoids provides information about plant stress, and its capacity to endure it [26]. Given our results, a specific quantification of the different carotenoids during esca development could not only be used for diagnostic purposes, but also for understanding some basic physiological processes induced by esca in the plant resulting in foliar symptoms. Previous studies that have looked at the total content of carotenoids in presymptomatic leaves did not see any statistically significant change, although at presymptomatic stages, some important physiological processes are strongly affected [27].

IV. Conclusion

This article reports initial encouraging findings that allow to identify symptomless leaves in esca-affected vines belonging to a diseased vine through a change in spectroscopic properties measured by RS likely due to a change in carotenoids. Such finding has a potentially high impact, because it could be extended to presymptomatic vines, and it would be the first example of early detection of a disease of complex/uncertain etiology, where no other methodology is available. The predictive value of RS in esca detection in the open field will be the subject of future research, monitoring a number of vines from the early vegetation stage throughout the whole season, until harvest; this will allow to increase the statistic sample and obtain a more robust model. Furthermore, the specificity of the response we here describe must still be evaluated in the context of typical abiotic and biotic stress commonly occurring in vineyards (drought, downy mildew, powdery mildews, yellows phytoplasma, leafroll viruses, and so on). At this stage, we cannot exclude that our RS marker is general or common for a number of stressors. Early detection could bring to specific vine-tailored interventions that could save individual vines (e.g., through trunk injection of endotherapeutics), a cornerstone of precision agriculture.

References

[1] C. Bertsch et al., "Grapevine trunk diseases: Complex and still poorly understood," *Plant Pathol.*, vol. 62, no. 2, pp. 243–265, Apr. 2013.

[2] V. Hofstetter, B. Buyck, D. Croll, O. Viret, A. Couloux, and K. Gindro, "What if esca disease of grapevine were not a fungal disease?" *Fungal Diversity*, vol. 54, no. 1, pp. 51–67, May 2012.

[3] G. Surico, L. Mugnai, and G. Marchi, "Older and more recent observations on esca: A critical overview," *Phytopathol. Mediterr.*, vol. 45, no. 1, pp. 68–86, 2006.

[4] P. R. G. Elena and E. Bruez, "Field suppression of Fusarium wilt disease in banana by the combined application of native endophytic and rhizospheric bacterial isolates possessing multiple functions," *Phytopathol. Mediterr.*, vol. 54, no. 2, pp. 241–252, 2015.

[5] P. Letousey et al., "Early events prior to visual symptoms in the apoplectic form of grapevine esca disease," *Phytopathology*, vol. 100, no. 5, pp. 424–431, May 2010.

[6] J. Fischer, S. J. Beckers, D. Yiamsawas, E. Thines, K. Landfester, and F. R. Wurm, "Targeted drug delivery in plants: Enzyme-responsive lignin nanocarriers for the curative treatment of the worldwide grapevine trunk disease esca," *Adv. Sci.*, vol. 6, no. 15, 2019, Art. no. 1970091.

[7] S. Di Gennaro et al., "Unmanned aerial vehicle (UAV)-based remote sensing to monitor grapevine leaf stripe disease within a vineyard affected by esca complex," *Phytopathol. Mediterr.*, vol. 55, no. 2, pp. 267–275, 2016.

[8] S. Yeturu, P. V. Jentzsch, V. Ciobotă, R. Guerrero, P. Garrido, and L. A. Ramos, "Handheld Raman spectroscopy for the early detection of plant diseases: Abutilon mosaic virus infecting Abutilon sp." *Anal. Methods*, vol. 8, no. 17, pp. 3450–3457, 2016.

[9] N. Altangerel et al., "*In vivo* diagnostics of early abiotic plant stress response via Raman spectroscopy," *Proc. Nat. Acad. Sci. USA*, vol. 114, no. 13, pp. 3393–3396, Mar. 2017.

[10] L. Sanchez, S. Pant, K. Mandadi, and D. Kurouski, "Raman spectroscopy vs quantitative polymerase chain reaction in early stage huanglongbing diagnostics," *Sci. Rep.*, vol. 10, no. 1, pp. 1–10, Dec. 2020.

[11] V. Egging, J. Nguyen, and D. Kurouski, "Detection and identification of fungal infections in intact wheat and sorghum grain using a hand-held Raman spectrometer," *Anal. Chem.*, vol. 90, no. 14, pp. 8616–8621, Jul. 2018.

[12] L. Mandrile et al., "Nondestructive Raman spectroscopy as a tool for early detection and discrimination of the infection of tomato plants by two economically important viruses," *Anal. Chem.*, vol. 91, no. 14, pp. 9025–9031, Jul. 2019.

[13] L. Mandrile et al., "Raman spectroscopy applications in grapevine: Metabolic analysis of plants infected by two different viruses," *Frontiers Plant Sci.*, vol. 13, Jun. 2022, Art. no. 917226.

[14] A. A. Gitelson and M. N. Merzlyak, "Signature analysis of leaf reflectance spectra: Algorithm development for remote sensing of chlorophyll," *J. Plant Physiol.*, vol. 148, nos. 3–4, pp. 494–500, 1996.

[15] A. H. Elmetwalli and A. N. Tyler, "Estimation of maize properties and differentiating moisture and nitrogen deficiency stress via ground-based remotely sensed data," *Agricult. Water Manage.*, vol. 242, Dec. 2020, Art. no. 106413.

[16] H. M. Kalaji, K. Bosa, J. Kościelniak, and Z. Hossain, "Chlorophyll *a* fluorescence—A useful tool for the early detection of temperature stress in spring barley (*Hordeum vulgare* L.)," *OMICS, J. Integrative Biol.*, vol. 15, no. 12, pp. 925–934, Dec. 2011.

[17] N. Altangerel, P.-C. Huang, M. V. Kolomiets, M. O. Scully, and P. R. Hemmer, "Raman spectroscopy as a robust new tool for rapid and accurate evaluation of drought tolerance levels in both genetically diverse and near-isogenic maize lines," *Frontiers Plant Sci.*, vol. 12, pp. 1–10, Jul. 2021.

[18] L. Lu, L. Shi, J. Secor, and R. Alfano, "Resonance Raman scattering of β-carotene solution excited by visible laser beams into second singlet state," *J. Photochemistry Photobiol. B, Biol.*, vol. 179, pp. 18–22, Feb. 2018.

[19] D. Ballabio and V. Consonni, "Classification tools in chemistry. Part 1: Linear models. PLS-DA," *Anal. Methods*, vol. 5, no. 16, pp. 3790–3798, 2013.

[20] K. Shin and H. Chung, "Wide area coverage Raman spectroscopy for reliable quantitative analysis and its applications," *Analyst*, vol. 138, no. 12, pp. 3335–3346, 2013.

[21] P. H. C. Eilers, "A perfect smoother," *Anal. Chem.*, vol. 75, no. 14, pp. 3631–3636, 2003.

[22] P. H. C. Eilers, "Parametric time warping," *Anal. Chem.*, vol. 76, no. 2, pp. 404–411, Jan. 2004.

[23] R. Baranski, M. Baranska, and H. Schulz, "Changes in carotenoid content and distribution in living plant tissue can be observed and mapped in situ using NIR-FT-Raman spectroscopy," *Planta*, vol. 222, no. 3, pp. 448–457, Oct. 2005.

[24] M. Baranska, M. Roman, J. C. Dobrowolski, H. Schulz, and R. Baranski, "Recent advances in Raman analysis of plants: Alkaloids, carotenoids, and polyacetylenes," *Current Anal. Chem.*, vol. 9, no. 1, pp. 108–127, Dec. 2012.

[25] H. Schulz, M. Baranska, and R. Baranski, "Potential of NIR-FT-Raman spectroscopy in natural carotenoid analysis," *Biopolymers*, vol. 77, no. 4, pp. 212–221, 2005.

[26] M. Magnin-Robert et al., "Leaf stripe form of esca induces alteration of photosynthesis and defence reactions in presymptomatic leaves," *Funct. Plant Biol.*, vol. 38, no. 11, pp. 856–866, 2011.

[27] P. Goufo and I. Cortez, "A lipidomic analysis of leaves of esca-affected grapevine suggests a role for galactolipids in the defense response and appearance of foliar symptoms," *Biology*, vol. 9, no. 9, pp. 1–24, 2020.

Camilla Baratto (Member, IEEE) received the M.S. *(cum laude)* degree in physics from the University of Parma, Parma, Italy, in 1997, and the Ph.D. degree in material science from the University of Brescia, Brescia, Italy, in 2022.

She is a Senior Researcher with the National Research Council–National Institute of Optics (CNR-INO), Brescia, Italy. She has authored or coauthored 74 articles on International Journals with referee. Her H-index is 29 (source ISI-2022). She has written three book chapters. Her research interests include conductometric and optically addressable gas sensors, continuous wave photoluminescence and Raman spectroscopy, preparation and characterization of gas sensors of nanostructured metal oxides, characterization of metal oxides (1-D) nanowires and nanostructures, and characterization of 2-D materials.

Dr. Baratto is a Topical Editor of the IEEE SENSOR JOURNAL.

Gina Ambrosio received the degree in physics from the La Sapienza University of Rome, Rome, Italy, in 2015, and the joint Ph.D. degree in science and physics from Katholieke Universiteit Leuven (KU Leuven), Leuven, Belgium, and the Catholic University of the Sacred Heart, Brescia, Italy, in 2020. The Ph.D. dissertation was on the electronic properties and the charge transfer processes between graphene and organic molecules.

She is currently a Postdoctoral Researcher with the National Research Council–National Institute of Optics (CNR-INO), Brescia, where she is involved in the projects HUB-sPATIALS3. She is skilled in working with photoluminescence, photoemission and Raman spectroscopy, scanning tunneling microscopy, synchrotron radiation, and magnetron sputtering for material growth. She has authored five publications – four as the first author (http://orcid.org/0000-0002-6003-614X) – and she presented her research work at national and international conferences.

Dr. Ambrosio received the best oral contribution from the Graphene2019 conference in Rome.

Guido Faglia was born in 1965. He received the MSS (*cum laude*) degree in electronics from the Polytechnic University of Milan, Milan, Italy, in 1991, and the Ph.D. degree in semiconductor gas sensors from the University of Brescia, Brescia, Italy, in 1996.

In 1993, he was appointed as an Assistant Professor with the Gas Sensor Laboratory, University of Brescia, where he has been an Associate Professor of Experimental Physics since 2000. He is involved in the study of preparation of metal–oxide–semiconductors (MOS) as thin films and quasi-monodimensional nanostructures for gas sensing, energy (solar cells and thermoelectrics), optoelectronic applications (LEDs), and nanomedicine. He has been involved in the European Commission Projects since 1992.

Dr. Faglia was a recipient of the Italian Full Professorship habilitation as excellent in Condensed Matter Physics 02/B1 in 2013.

Massimo Turina received the M.S. degree in plant pathology and the Ph.D. degree in plant virology from the University of Bologna, Bologna, Italy, in 1993 and 1998, respectively.

He was a Post Doctoral Research Associate (PDRA) with Texas A&M University, College Station, TX, USA, and with the University of California at Davis, Davis, CA, USA, from 1999 to 2002. He is currently a Senior Researcher with the National Research Council (CNR), Institute for Sustainable Plant Protection, Turin, Italy. He is also the Head of the Department of Molecular and Translational Medicine, University of Brescia, Brescia, Italy. Since 2002, he has been with the National Research Council, Plant Virology Institute (currently Institute for Sustainable Plant Protection). Recently, he coordinated the H2020 RIA-SFS17 project. He has authored more than 130 articles indexed in Web of Science (WoS) and Scopus, and has an H-index of 30 in WoS. He has written three book chapters. He has coauthored two patents. His main research interests include plant disease diagnostic and characterization, the molecular aspects of virus–plant host interactions, and mycovirus–host interactions.

Dr. Turina is a member of the editorial board of Environmental Microbiology and Virus Research, and the Mymonaviridae, Botourmiaviridae, and Tospoviridae working groups. He is the Head of the Hypoviridae Working Group, International Committee for the Taxonomy of Viruses (ICTV). He is an Editor of the *Archives of Virology*.

Open Access funding provided by 'Consiglio Nazionale delle Ricerche-CARI-CARE' within the CRUI CARE Agreement